Photoionization Yield vs Energy in H_2O and D_2O

David M. Bartels* and Robert A. Crowell

Argonne National Laboratory, Chemistry Division Building 200, Argonne, Illinois 60517

Received: November 22, 1999; In Final Form: January 21, 2000

A simple conductivity jump method was used to measure the escaped solvated electron yield following two-photon excitation of water with Raman-shifted light from an amplified mode-locked Nd:YAG laser. Between 7.8 and 9.3 eV, the quantum efficiency for the escape yields changes from 1.9% to 22%, with an almost exponential dependence on the excitation energy. Quantum efficiency in D_2O is smaller and resembles the H_2O behavior at 0.35 eV lower energy. The quantum yield measured for one-photon excitation near the water absorption edge at 6.4 eV is a surprisingly large 1.3%. We propose that the mechanism for low energy photoionizaton of water is best described as a dissociative proton-coupled electron transfer to a preexisting trap.

Introduction

Since the work of Boyle et al.[1] was published in 1969, it has been known that one can generate solvated electrons in neat water with relatively low energy UV photons. Anbar et al.[2] reported a measurable yield virtually from the water absorption edge near 6 eV. Given the 12.6 eV ionization potential of H_2O vapor, this represents an astonishing 6.6 eV reduction in the "ionization potential" of water. It was noted immediately[1] that the stoichiometry of the process

$$H_2O \rightarrow (e^-)_{aq} + OH + (H^+)_{aq} \qquad (1)$$

is characterized by a free energy change of $\Delta G = 5.8$ eV so that it might be driven with photon energies near the liquid absorption edge. It was not remarked until more recently that the ionization process must "compete" on a femtosecond time scale with direct dissociation of a water molecule from the unbound $A(^1B_1)$ electronic surface to form OH radicals and H atoms.[3] Though several reviews have been written to examine the relevant data,[3−6] it remains unclear exactly how the ionization at very low energy occurs.

In recent years, multiphoton ionization of water with picosecond and femtosecond lasers has been applied to learn about the yield and geminate recombination kinetics of solvated electrons for excitation energies above 7.8 eV.[7−18] Work in our laboratory demonstrated that for two-photon excitation between 7.8 and 9 eV, there is no change in the geminate recombination kinetics of the solvated electron−roughly 45% escape.[7,8] Thomesen et al.[18] recently obtained the same escape yield at 9.3 eV. These studies confirmed that the ionization does not occur through a quasi-free conduction band electronic state, because additional energy should result in greater distance between geminate partners and corresponding greater escape yield. Rather, localized electronic states must be involved. Whereas the geminate escape fraction is virtually constant, the quantum yield was shown by Nikogosyan et al.[10] to decrease exponentially from 9.3 to 7.8 eV. This means that the efficiency to generate solvated electrons in the first picosecond is a strong function of excitation energy. It was suggested that this should correlate with an Urbach tail of the water conduction band.[19] In the present study we have measured the escape yield of solvated electrons to confirm the results of Nikogosyan et al.[10] and to examine the effect in D_2O. Comparison is also made with one photon ionization at 6.4 eV. In our discussion, we examine the mechanistic details and propose that the best description is a photoinitiated dissociative proton-coupled electron transfer.[20]

Experimental Section

The yield measurement is accomplished by scavenging solvated electrons with dissolved SF_6, which proceeds to hydrolyze with the overall stoichiometry[21]

$$(e^-)_{aq} + SF_6 \rightarrow HSO_3^- + 6F^- + 6H^+ + OH \qquad (2)$$

The ionic products produce a large change in conductivity which is readily detected.

According to the time-resolved conductivity study of Asmus et al.[21] the chemistry proceeds to completion in well under one millisecond. The initial reaction proceeds with a near-diffusion-controlled rate of 1.5×10^{10} M^{-1} s^{-1}.[21] A time-resolved absorption experiment in our laboratory confirmed that the electron lifetime in a saturated SF_6 solution is roughly 300−500ns, so that scavenging does not significantly interfere with the geminate kinetics in the first nanosecond. Second-order recombination chemistry is not important on this time scale for the focusing conditions used.

The conductivity cell was constructed by modifying a 50 mL Erlenmeyer flask to add suprasil fused silica windows and conductivity electrodes. A filling tube with a ground-glass joint was connected near the flask bottom. The top of the flask was sealed with a latex septum, so that syringe needles could be used to control the inert gas pressure over the sample. The removable 1 mm thick windows were sealed with viton O-rings. The optical path length was approximately 8 cm. The electrodes were held in the flask approximately 1 cm apart, and standardization of the cell with KCl solution gave a cell constant of 0.163 cm^{-1}.

Ultrapure 18.3 Mohm−cm water for the experiments was obtained directly from a Barnstead Nanopure four-cartridge system which in turn took water from a building deionized water system. Residual organic impurities from the cartridge system

10.1021/jp9941460 CCC: $19.00
Published on Web 03/24/2000

were at the level of 12 ppb total organic carbon, as measured with an on-line TOC monitor. An ca. 400 mL glass bubbling jar was first purged with argon, then filled directly from the Nanopure system to avoid contamination by CO_2. The water was bubbled for ca. 15 min with argon and/or SF_6 to remove oxygen, after which the conductivity cell was filled under the bubbling gas. In blank experiments with just Ar bubbling, conductivity changes induced by the laser were completely negligible. Approximately 30 mL of solution was used for a typical filling. The cell and solution were weighed to determine the actual solution volume at each filling. For D_2O experiments a similar procedure was followed, except that the cell was filled directly from a Nanopure cartridge system dedicated to heavy water. The sample was then bubbled with SF_6 through the filling port to purge oxygen.

Conductance was measured with a YSI model 35 conductivity meter (Yellow Springs Instruments, Inc.) set for 20 microsiemens full scale. The 0−2 V analogue output from this device was measured with an Hewlett-Packard 885 differential voltmeter whose chart-recorder output was digitized with a 12-bit A/D converter on a Macintosh II computer. Using the differential voltmeter, conductivity jumps of one nanosiemen were easily measured in the very pure water. Precision in the measurement was apparently limited by swirling of the sample needed to produce uniform concentration of ions, which could add or lose a few ions on the vessel wall.

To generate two-photon photolysis pulses, a mode-locked CW Nd:YAG laser (Coherent Antares) was used to seed a regenerative amplifier, which was triggered at 10 Hz repetition frequency. The output was doubled and quadrupled. The 266 nm fourth harmonic pulse was either used directly (after attenuation) or focused through an H_2 or D_2 cell for Raman shifting. A suprasil quartz prism was used for wavelength separation after recollimation of the light. Between 0.5 and 2 mJ/pulse could be obtained in the first three (Stokes-shifted) Raman orders.

The light exiting the conductivity cell was measured directly on a Molectron J25−170 pyroelectric detector which had just been calibrated at 266 nm. The black absorbing surface of this detector is designed to have response independent of wavelength. The Molectron company claims absolute accuracy and reproducibility of the calibration of better than 5%, which should be the ultimate accuracy in our experiment. In front of the cell a 3 mm fused silica wedged window was placed as a beam splitter to provide a relative I_o measurement. Care was taken to avoid significant 2-photon absorption in the beam splitter by not placing it too near the focus. The reflection from this splitter was focused onto a UV-transmitting diffuser in front of an EG&G FND100Q photodiode to provide the I_o measurement. Both the photodiode and the pyroelectric detector response were amplified with battery-powered operational amplifiers and then digitized and averaged on a Tektronix TDS 350 digital oscilloscope.

Measurement of the one-photon quantum yield at 193 nm was accomplished in much the same way using the pulse of a Lamda Physik LPX 100 ArF laser. The unfocused beam was apertured to approximately 3 mm diameter, and the ca. 5% front surface reflection from the suprasil beam splitter was used for the experiment. The linear absorption measured at 193 nm agreed well with the value reported by Quickenden and Irvin[19] for ultrapure water.

The procedure for each measurement was as follows: First, several hundred laser shots were averaged on the digital oscilloscope with the conductivity cell absent. This provided a calibration for the I_o measurement in this geometry based on the calibration of the pyroelectric detector, whose response is essentially independent of beam geometry over its 27 mm diameter active area. The ratio of I_t/I_o had a standard deviation of 0.5% or better under the conditions used for experiments, where Raman shifted pulse amplitudes had ca. 20% standard deviation. The conductivity cell was then put into place, and the computer began recording the baseline of the conductivity cell. After ca. 10 s, some appropriate number (10−250) of laser shots were fired through the cell; the I_o and I_t signals for all of the shots were averaged on the digital oscilloscope. Immediately after the laser finished, the cell was picked up and the solution was swirled vigorously to produce a homogeneous solution of the product ions. The final conductivity change was measured within a few seconds after the solution settled. The total absorption of light in the water is calculated from $(1 - R)I_o - I_t/(1 - R)$ where R is the normal incidence reflection loss at the air/fused silica interface for the wavelength in use. Losses at the water/silica interface were too small to make a difference.

Conversion of conductivity jump to solvated electron yield was made assuming the stoichiometry of eq 2. At 25 °C, equivalent conductivites for F^- and HSO_3^- ions are 54.7 and 50 Siemen cm^2/mole, respectively.[22] These numbers were corrected for temperature (recorded during each measurement) by dividing by the ratio of viscosities $\eta(t)/\eta(25)$. A similar assumption (conductivity proportional to viscosity) was made to correct the specific conductivities of these ions for heavy water. Proton and deuteron conductivities in H_2O and D_2O respectively were calculated from the equations[23]

$$\lambda(H^+) = 224.33 + 5.305t - 0.0113t^2 \quad (3)$$

$$\lambda(D^+) = 148.35 + 4.320t - 0.0098t^2 \quad (4)$$

where λ is in Siemen cm^2/mole and t is temperature in degrees Celsius. From the conductivity jump, the cell constant, the total solution volume, and the specific conductivities for the product ions an absolute number of scavenging events can be deduced. Division by the total number of photons absorbed gives the (escape) quantum yield of solvated electrons.

Results

To discuss our results and compare with other work, we need to carefully define our terms. Nikogosyan et al.[10] defined their quantum yields in terms of the solvated electrons produced per one photon, even though two photons were absorbed per quantum event. We prefer the term quantum efficiency, which is the normal quantum yield for one-photon events, or the yield per two photons when we are discussing two-photon excitations. We will take pains to specify whether we are referring to an initial quantum yield (production of solvated electrons in the first picosecond) or an escape quantum yield which is what we are able to measure by scavenging. For the excitation range 9.3−7.8 eV the two are proportional because of the energy-independent geminate recombination.[7]

Final results of a typical data set for 319 nm are shown in Figure 1. To be confident in the yield measurement, we plot the apparent yield vs the fraction of light absorbed in the cell. As noted by Nikogosyan et al.,[10] prompt absorption by the $(e^-)_{aq}$ and OH radical products can attenuate the pump beam without giving any additional ionization. At higher pump intensities (larger fraction absorbed) this shows up as a decrease in the apparent yield. It was difficult to change the intensity of the Raman-shifted pulses by attenuating the pump power. Instead, the light was gently focused with either a 75 cm or 50 cm lens, and the cell was moved by several centimeters relative to the

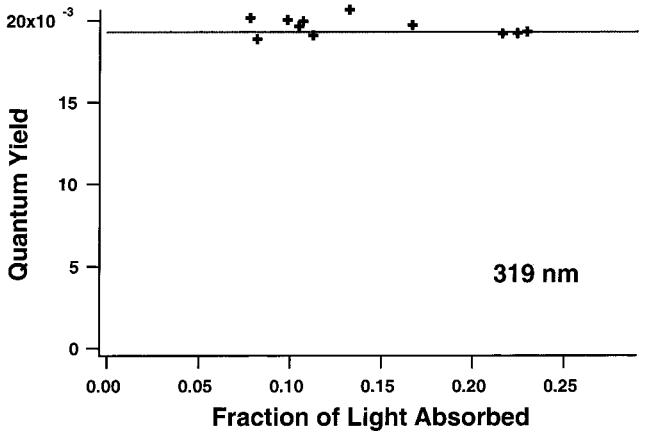

Figure 1. Quantum yield results for H_2O and 319 nm Raman-shifted light. The fraction of light absorbed was changed by shifting the cell with respect to the laser focus so that the average intensity in the sample changed. The individual data points represent integration of 200 or 250 laser shots.

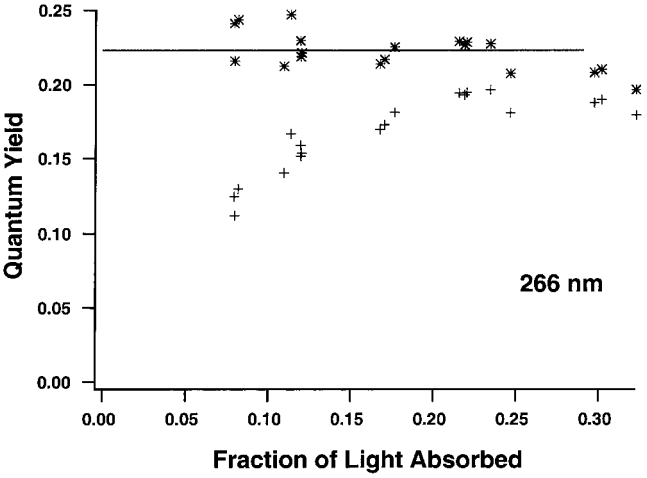

Figure 2. Apparent quantum yield (+) for solvated electrons in H_2O, with two-photon excitation at 266 nm. Corrected for additional linear loss of photons (*).

focus to change the average effective intensity. Errors in the measurement are dominated by uncertainty in the light absorption, especially as the fraction absorbed becomes smaller than 10%.

Figure 2 shows the results for 266 nm. At higher laser power, with fractions of 30% or more absorbed in the water, the yield falls due to product (OH radical, $(e^-)_{aq}$) absorption of part of the laser pulse. The apparent decrease in yield below about 20% absorbed was unexpected, but quite reproducible in both H_2O and D_2O, and with chlorocarbon scavengers (producing HCl product) as well as the SF_6. In the case of the 266 nm light, no focus was necessary to obtain large absorptions. To attenuate the beam, neutral density filters were employed in the 532 nm doubled light. In Figure 3 we plot the fraction of light absorbed vs the incident energy for an ca. 3 mm diameter beam. This plot is linear as expected for a pure two-photon absorption, but does not extrapolate to the origin. Thus, both the yield and absorption measurements seem to indicate an additional one-photon loss mechanism which accounts for ca. 4−5% of the light. The cell windows were checked in a spectrophotometer, and no hint of absorption could be found. The "linear loss" behavior was not indicated at longer wavelengths. The missing light corresponds to an absorption of about 2.8×10^{-3}/cm in the 8 cm path, which is an order of magnitude larger than the absorption measured by Quickenden and Irvin at 266 nm.[24] We

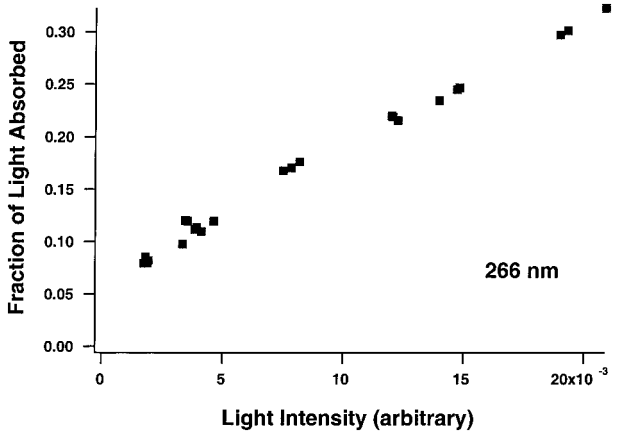

Figure 3. Fraction of light absorbed at 266 nm vs the transmitted light intensity measured on the pyroelectric detector. Linear behavior is expected for two-photon absorption, but the nonzero intercept indicates an additional linear loss mechanism.

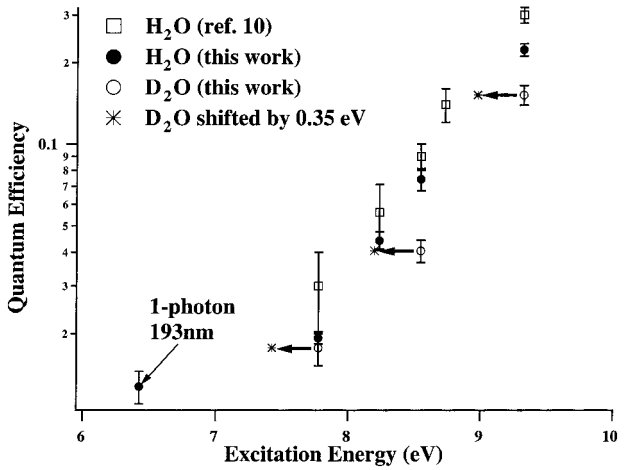

Figure 4. Semilog plot of quantum efficiencies for solvated electron escape measured in the present study and by Nikogosyan et al.[7]

TABLE 1: Escape Quantum Yields for Hydrated Electrons

excitation energy	H_2O	D_2O
9.32 eV	0.223 ± 0.011	0.152 ± 0.013
8.55 eV	0.074 ± 0.007	0.040 ± 0.004
8.23 eV	0.044 ± 0.004	
7.78 eV	0.019 ± 0.001	0.018 ± 0.002
6.42 eV	0.0127 ± 0.0017	

can only surmise that the loss is either due to an organic impurity introduced in the filling procedure (unlikely), or perhaps due to scattering by particulate matter in the cell. The yield can be corrected for the additional loss mechanism, as indicated in Figure 2, and results fall into line with the data from other wavelengths (and the earlier study of Nikogosyan et al.[10]).

One measurement at the first anti-stokes line of D_2 (245 nm) was attempted, but the product absorption, and probably, linear loss problems were more severe. The limited light intensity did not allow us to carefully explore the intensity dependence. We can confirm, however, that the quantum efficiency is still higher ($\geq$0.3) at this shorter wavelength.

The quantum efficiency results found in this study are tabulated in Table 1 and plotted vs excitation energy in Figure 4, along with the earlier transient conductivity results of Nikogosyan et al.[10] The two studies clearly agree within a calibration scaling factor. The present study provides more precision at the lower excitation energies because multiple shots could be averaged. The one-photon quantum yield at 193 nm

(6.4 eV) agrees with the report of Iwata et al.,[25] that the "quantum yield of ionization was a few percent". We are also in agreement with the original report of Boyle et al.,[1] who estimated a quantum yield on the order of 0.005 near the absorption edge (but who suggested that the threshold for ionization was 6.5 eV). We differ with the report of Anbar et al.,[2] who used the same SF_6 scavenger, but reported a larger 7.7% ionization yield (in the presence of 0.1 M methanol which might have absorbed much of the light).

Discussion

The quantum efficiencies found in this study are plotted logarithmically vs excitation energy in Figure 4. Several salient features of this plot will form the basis for our discussion. Both the H_2O and D_2O data in the 7.8−9.3 eV region follow an exponential behavior. The smaller D_2O yields look very much like the H_2O results, shifted by 0.35 eV in excitation energy. The one-photon quantum yield at 6.4 eV emphatically does not fit this exponential dependence, being some five times too large. Finally, we note that the ionization efficiencies are quite large. The numbers plotted are escape efficiencies, and our previous work[7,8] showed that the fraction of geminate recombination was approximately 0.55 in this energy range. Thus, the initial (i.e., in the first picosecond) quantum efficiency to produce solvated electrons with 9.3 eV excitation is approximately $0.22/(1.0 - 0.55) = 0.49$.

Goulet et al.[19] first suggested that the exponential dependence of the yield on excitation energy in the 7.8−9.3 eV regime represents a correlation with the "Urbach tail" of the conduction band. (Geminate recombination results indicate that the conduction band is reached starting with about 9.5 eV excitation.[7]) The Urbach tail represents a distribution of "preexisting sites" in which an electron with given total energy might be localized.[26−29] The idea is that water is excited to a "localized exciton" state, which either dissociates to H and OH, or decays by transfer of an electron to the preexisting trap. We have suggested that this could explain the energy-independent geminate recombination kinetics,[7,8] because the distance reached between the newly solvated electron and its geminate partners is limited by the relatively small range of electron transfer which is possible on a femtosecond time scale. Depending on the energy available in the excitation event, the electron may not be close enough to a trap of sufficient depth, and the electron transfer may not occur. The density of trap sites which can support an electron of a given energy is expected to follow an exponential dependence.[19,26−29]

To confirm the feasibility of this mechanism, we should calculate the total density of trap sites required by the data. The efficiency for prompt formation of solvated electrons is about 50% at 9.3 eV as we noted above. The average initial distance between the electron and its geminate partners is about 1 nanometer, based on simulations of the geminate recombination kinetics.[7,8,18] This implies that 50% of all water molecules have at least one trap site within about 1 nm. A sphere of 1 nanometer radius centered on any trap site would include about 130 water molecules in a volume of 4×10^{-24} liters. We calculate that traps must be present at a concentration of roughly 0.2 mol/liter in order to include 50% of the total volume. From analysis of molecular dynamics simulations Hilczer and Tachiya[27] calculate a concentration of about 0.4 M preexisting traps in methanol, and a similar concentration seems likely for water.[30] Motakabbir et al.[29] estimated a lower value of 0.01 M traps in water using different criteria. Obviously our estimate could be reduced by an order of magnitude if a slightly larger radius were used. Nevertheless, if we accept an "electron transfer to preexisting trap" mechanism, we must be prepared to account for its extreme efficiency. Exciton hopping might be invoked to explain part of the efficiency, if exciton traps are often located near preexisting electron traps. This idea might well have merit because the condensed phase water $A(^1B_1)$ spectrum is so strongly blue-shifted relative to the vapor. Water molecules located near voids (good electron traps) might be expected to absorb further to the red and so act as exciton traps.

Goulet et al.[19] also pointed out that photoionization data for indole and tryptophane exhibit an exponential decrease with excitation energy, but the slope is very different from water. The water behavior in Figure 4 is described (for quantum efficiency Ø) with $d(\ln Ø)/dE = 1.6\ eV^{-1}$, but the indole and tryptophane slopes are ca. $4.5\ eV^{-1}$.[19] It was suggested that the slopes are due to different final electronic states, but no clues were given as to what these might be. Simulations of excess electron wave functions in unperturbed water by Motakkabir and Rossky[28] seem to indicate that the trap density (i.e., occurrence of localized electron wave functions with particular energy) should fall off with logarithmic slope of roughly $3-5\ eV^{-1}$.[31] A similar falloff in trap density with energy seems to apply in the methanol simulations of Hilczer and Bartczak.[26] These simulations are immediately consistent with the interpretation of Goulet et al. for the aromatic photoionization data, but not with the water data.

We believe that the photoinduced electron-transfer idea proposed by Goulet et al.[19] is essentially correct, but their explanation is incomplete in several respects. In 1997 Coe et al.[32] published a complete reevaluation of the water "vacuum level", "conduction band edge", and "band gap" energetics, being very careful to derive *adiabatic* (i.e., thermodynamic average) energies for the electron *and its counterion*. The importance of reorganization energy (i.e., solvation of the counterion or trap site) was emphasized in the interpretation of photoemission threshold experiments because, depending on fluctuations in the local environment, vertical (Born−Oppenheimer) transition energies may deviate from the average by an entire electronvolt. This fact has large implications for the water photoionization problem. As a first-order approximation, the exponential slope for water photoionization in the 7.8−9.3 eV range is a product of the density distribution for electron trap sites, multiplied by the distribution in "preexisting cation solvation energies" which is accessed by the absorption spectrum. A shallow electron trap can be paired with a very favorable cation environment to improve the probabilities at low photon energies. This explains the logarithmic slope difference between water and the aromatic solutes. The solvation energies of the aromatic cations are relatively well-defined, and the quantum efficiency slope is determined mostly by the solvent electron trap density.

A first quantum calculation of the liquid water absorption spectrum has now been accomplished by Bursulaya et al.[33] using a truncated adiabatic basis set molecular dynamics simulation,[34] and a similar picture emerges of the large site-to-site variation in solvation energy. A single sharp transition energy in the isolated molecule is dramatically blue-shifted and broadened by on the order of 0.5 eV due to the large dispersion in local electric field. The extreme red tail of the absorption spectrum is identified with the extreme in the distribution of local electric field. If this is correct, it suggests that light absorption in the red tail of the spectrum preferentially selects those water molecules which are in very favorable environments for cation solvation. This explains nicely the relatively high quantum yield

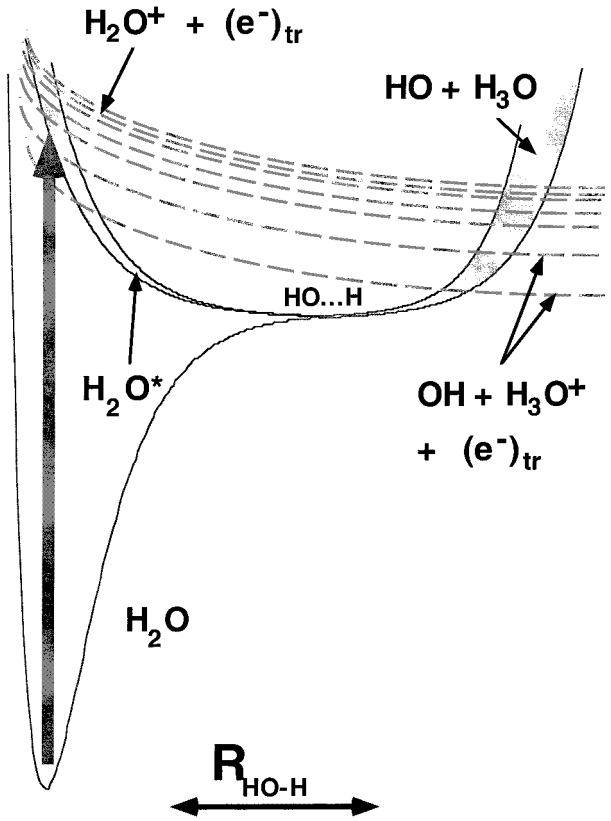

Figure 5. Potential energy diagram for the low-energy photophysics of liquid water projected onto the HO···H degree of freedom. The H_2O $A(^1B_1)$ state dissociates to (HO···H) as in the gas phase, but H immediately runs into another water molecule, which is the H_3O repulsive potential on the right. In the event that a suitable trap site for an electron is nearby, ionic surfaces (dashed lines) cross the neutral potential.

for solvated electrons measured near the water absorption threshold at 6.4 eV.

The recognition of large dispersion in counterion solvation energy is still not the entire explanation of low-energy water photoionization. We have emphasized,[3,7,8] along with other workers,[4] that a proton transfer is essential in allowing the ionizaton to occur at the very lowest photon energies. Proton transfers and electron transfers are the only processes which can compete kinetically with the dissociation of water to H and OH, which should otherwise occur in a single vibrational period. In Figure 5 we plot the potential energy surfaces of liquid water projected along the HO−H degree of freedom. The shaded region on the excited surface represents the distribution in transition energies induced by local electric field perturbations. We presume that just as in the vapor, the $A(^1B_1)$ excited state is dissociative. By simple conservation of momentum, 95% of the excess energy should go into H atom translation, producing a kinetically hot atom. In the liquid, though, the nascent H atom immediately encounters the adjoining hydrogen-bonded oxygen atom. The H_3O potential indicated on the right of Figure 5 is presumed to be purely repulsive. Crossing this neutral potential energy surface there may be ionic surfaces, as indicated by the dashed lines in the figure. If a favorable electron trap is immediately available, an electron transfer may occur to leave behind the H_2O^+ ion. But the proton transfer

$$H_2O^+ + H_2O \rightleftharpoons HO + H_3O^+ \qquad (5)$$

is exothermic in the gas phase by about 1.0 eV.[35] The ionic surfaces in the figure are therefore slanted down toward the right, where the state would be described as an $HO\cdots H_3O^+$ pair, with the electron in a nearby trap site. The important insight to be gained from this figure, is that the energy available for an electron tranfer is changing on the order of an electronvolt as the water dissociation occurs. At some point on this R_{HO-H} coordinate, energy matching required for an electron transfer should be satisfied if there are any traps nearby. The process we are suggesting could be called a photoinduced, dissociative proton-coupled electron transfer.[20]

We now consider how the H_2O/D_2O isotope effect fits into this picture. The geminate kinetics in D_2O are different from H_2O, but we have shown that below 9 eV, most of this difference is due to the isotope effect on diffusion coefficients.[7] The smaller reactivity of $(D^+)_{aq}$ than $(H^+)_{aq}$ for solvated electrons results in approximately 3% greater escape fraction in D_2O. This is much too small, and in the wrong direction, to explain the isotope effect in Figure 4, and we can safely ignore it. An isotope effect which must be accounted for is the vibrational zero point energy of the ground state water molecule, which is 0.16 eV lower in D_2O. The absorption threshold of heavy water is blue shifted by this amount relative to light water.[36] To correct for this we should shift the D_2O excitation energy to the left in Figure 4 as indicated. However, 0.16 eV falls short of the 0.35 eV shift required to match the light water yields. After shifting the energy scale by 0.16 eV, the D_2O escape yields are still about 30% below the (interpolated) H_2O yields. (Note that our comments here do not apply to D_2O excited with 7.8 eV, which seems to fall into the lower energy regime where quantum yield does not change much with excitation energy.)

If a simple correlation with preexisting trap sites were to explain the isotope effect, the data seem to indicate that the distribution of trap depths is shifted by about 0.19 eV, leaving 30% fewer traps of a given energy in D_2O. Virtually all of the structural properties of D_2O at a temperature T are similar to those of H_2O at about $(T - 7)$ degrees.[37] A simple correlation with preexisting traps would imply that changing the temperature of water by about seven degrees should change the density of traps, and corresponding hydrated electron yields, by about 30%. This would represent a very large temperature effect on a purely equilibrium structural property, and we believe this explanation for the isotope effect must be rejected. For comparison, the absorption edge of water in the 6.7 eV region red-shifts only 0.12 eV when changing from 24 °C to 80 °C.[38]

The zero point energy change in the proton transfer could play a role, but the primary isotope effect is too small and in the wrong direction: an OD bond of D_3O^+ will be more stable than an OH bond of H_3O^+, leaving more electronic energy for electron transfer in heavy water. It seems most likely that the remaining isotope effect represents a dynamic effect: the more rapidly reorienting H_2O molecules solvate both the cation and the electron more efficiently in competition with a recombination process. Although we emphasize the proton transfer in Figure 5, other solvent degrees of freedom also participate.

Finally, we consider the merits of two other mechanisms which have been proposed to explain the low energy ionization. In our previous work[7] we suggested that the ionization might be the result of hot H atom chemistry. The dissociation energy for a water OH bond is 5.1 eV, so in absorption of photons by water there is always in excess of 1 eV energy which should end up in H atom translation. In high-temperature water, it is known that H atoms react with H_2O giving solvated electrons and hydronium ions

$$(H)_{aq} + H_2O \rightleftharpoons (e^-)_{aq} + (H_3O^+)_{aq} \quad (6)$$

The activation energy for reaction 6 is 0.75 eV, so a dissociating water molecule might immediately induce the hot H atom reaction. Consideration of Figure 5 shows that there is much in common between the "hot H atom" and the "proton-coupled electron transfer" ideas. The main difference is a description of where the electron localizes in reaction 6. We have argued[39] that for reaction 6 to occur thermally, the electron will localize in the (preexisting) hydrophobic solvation cavity of the H atom. In general such a cavity will not exist next to a dissociating water molecule. One could argue that the dissociation creates its own trap site. However, it is difficult to see how the average 1 nm distance between the electron and the OH radical can be accounted for by this mechanism. It is still interesting to contemplate the possible chemistry of "H_3O" on the right-hand side of Figure 5, but we feel water ionization is better described in terms of proton-coupled electron transfer.

Another description of the mechanism first proposed by Anbar et al.[2] and more recently discussed by Bernas and Grand[4] can be written

$$H_2O^* + H_2O \rightarrow OH^-{}^* + H_3O^+ \quad (7)$$

where the fundamental process is described as a proton transfer from the excited water molecule to its neighbor, leaving behind an electronically excited OH^- ion. The excited $OH^-{}^*$ then loses its electron as in a charge-transfer-to-solvent (CTTS) excitation.[40] There is formally little to distinguish this proposal from the proton coupled electron transfer pictured in Figure 5. In terms of recent theoretical treatments, this might be called a consecutive proton transfer, electron transfer (PT/ET) process.[20] However, several details of this description seem inadequate. First, the implication is that OH^- has a stable low-lying anion excited state, which does not exist in the gas phase. CTTS states only exist in water because of the large (preexisting) reaction potential induced by the negative charge itself,[40−44] and in the water excitation process the necessary alignment of dipoles has not yet occurred. Second, the analogy to CTTS excitation implies that the electron solvation is dominated by an adiabatic process, which ought to produce shorter initial distances than observed.[41−44] In Figure 5 we are deliberately vague as to where the electron trap is. To obtain average $OH-(e^-)_{aq}$ distances on the order of 1 nm in the first picosecond, without invoking delocalized or "conduction band" states, this seems to be essential. We also fail to understand how the adiabatic solvation idea should produce a quasi-exponential dependence of the quantum efficiency on excitation energy (7.8−9.3 eV). All of these objections to the description of water ionization by way of eq 7 are offered without conclusive evidence. Simulations of water photoionization similar to those performed for chloride ion[41,42] and iodide ion[43,44] would be valuable in this regard. It is interesting to note that electron transfer to a preexisting trap site was actually observed as a minor channel in the CTTS modeling study of Sheu and Rossky[43,44] for relaxation of higher energy states.

Summary

Using a simple conductivity technique, we have confirmed existing quantum yield results for two-photon ionization of light water between 9.3 and 7.8 eV excitation energy, and for one-photon ionization at 6.4 eV. After correcting for the energy-independent geminate recombination, quantum efficiency for solvated electron production in the first picosecond is roughly 50% at 9.3 eV, and falls exponentially with energy to about 4% at 7.8 eV. At 6.4 eV the efficiency is still at about 2.5%. We propose that these results can be explained in terms of a dissociative proton-coupled electron transfer mechanism. As the excited water molecule dissociates, it is possible to cross onto an ionic surface representing an electron in a "preexisting trap" site and a corresponding cation which may be either H_2O^+ in one limit, or an $(HO\cdots H_3O^+)$ pair at the other. This process remains quite efficient at rather low excitation energies because of the large distribution in "preexisting cation solvation" energies which can be found in water. In D_2O, efficiencies are ca. 30% lower after correcting for zero point energy, and we conclude that this stems from a dynamic effect in electron and cation solvation. In the red tail of the absorption spectrum, we postulate that the efficiency remains near 2.5% because the absorption selects those water molecules which have very favorable cation solvation environments.

Acknowledgment. This work was performed under the auspices of the Office of Basic Energy Sciences, Division of Chemical Science, US-DOE under contract number W-31-109-ENG-38. The authors would like to express their thanks to David Tiede and Arlene Wagner for providing the sample of purified D_2O. We thank Dr. Hyung Kim for providing a preprint of his spectral modeling results, and Dr. Maria Hilczer for communication of unpublished results. We thank Dr. James Coe, Dr. Peter Rossky, and Dr. Soren Keiding for useful discussions.

References and Notes

(1) Boyle, J. W.; Ghormley, J. A.; Hochanadel, C. J.; Riley, J. F. *J. Phys. Chem.* **1969**, *73*, 2886.
(2) Anbar, M.; St. John, G. A.; Gloria, H. R.; Reinisch, R. F. In *Water Structure at the Water−Polymer Interface*; Jellinek, H. H. G., Ed.; Plenum Press: New York, 1972, 85.
(3) Han, P.; Bartels, D. M. *J. Phys. Chem.* **1990**, *94*, 5824.
(4) Bernas, A.; Grand, D. *J. Phys. Chem.* **1994**, *98*, 3440.
(5) Sander, M. U.; Luther, K.; Troe, J. *Ber. Bunsen-Ges. Phys. Chem.* **1993**, *97*, 953.
(6) Bernas, A.; Ferradini, C.; Jay-Gerin, J.-P. *Chem. Phys.* **1997**, *222*, 151.
(7) Crowell, R. A.; Bartels, D. M. *J. Phys. Chem.* **1996**, *100*, 17940.
(8) Crowell, R. A.; Bartels, D. M. *J. Phys. Chem.* **1996**, *100*, 17713.
(9) Crowell, R. A.; Qian, J. *J. Phys. Chem. A*, in press.
(10) Nikogosyan, D. N.; Oraevsky, A. A.; Rupasov, V. I. *Chem. Phys.* **1983**, *77*, 131.
(11) Sander, M. U.; Luther, K.; Troe, J. *J. Phys. Chem.* **1993**, *97*, 11489.
(12) Gauduel, Y.; Pommeret, S.; Migus, A.; Antonetti, A. *J. Phys. Chem.* **1991**, *95*, 533.
(13) Gauduel, Y.; Pommeret, S.; Migus, A.; Antonetti, A. *Chem. Phys.* **1990**, *149*, 1.
(14) Gauduel, Y.; Pommeret, S.; Migus, A.; Antonetti, A. *J. Phys. Chem.* **1989**, *93*, 3880.
(15) Migus, A.; Gauduel, Y.; Martin, J. L.; Antonetti, A. *Phys. Rev. Lett.* **1987**, *58*, 1559.
(16) Reuther, A.; Laubereau, A.; Nikogosyan, D. N. *J. Phys. Chem.* **1996**, *100*, 16794.
(17) Hertwig, A.; Hippler, H.; Unterreiner, A. N.; Voehringer, P. *Ber. Bunsen-Ges. Phys. Chem.* **1998**, *102*, 805.
(18) Thomsen, C. L.; Madsen, D.; Keiding, S. R.; Thogersen, J.; Christiansen, O. *J. Chem. Phys.* **1999**, *110*, 3453.
(19) Goulet, T.; Bernas, A.; Ferradini, C.; Jay-Gerin, J.-P. *Chem. Phys. Lett.* **1990**, *170*, 492.
(20) Cukier, R. I. *J. Phys. Chem.* A **1999**, *103*, 5989.
(21) Asmus, K.-D.; Gruenbien, W.; Fendler, J. H. *J. Am. Chem. Soc.* **1970**, *92*, 2625.
(22) *Landolt-Bornstein Zahlenwerte und Funktionen:* Vol. II, 7. Teil.; Springer-Verlag: Berlin, 1960; p 112ff.
(23) These equations are the complement of those for OH^- conductivity derived in an earlier publication: Schmidt, K. H.; Han, P.; Bartels, D. M. *J. Phys. Chem.* **1992**, *96*, 199.
(24) Quickenden, T. I.; Irvin, J. A. *J. Chem. Phys.* **1980**, *72*, 4416.
(25) Iwata, A.; Nakashima, N.; Izawa, Y.; Yamanaka, C. *Chem. Lett.* **1993**, 1939.
(26) Hilczer, M.; Bartczak, W. M. *J. Phys. Chem.* **1993**, *97*, 510.

(27) Hilczer, M.; Tachiya, M. *J. Phys. Chem.* **1996**, *100*, 7691.
(28) Motakabbir, K. A.; Rossky, P. *J. Chem. Phys.* **1989**, *129*, 253.
(29) Motakabbir, K. A.; Schnitker, J.; Rossky, P. J. *J. Chem. Phys*. **1992**, *97*, 2055.
(30) Preliminary results indicate 0.2 M traps in water using a similar method: Hilczer, M., personal communication.
(31) Figure 5 of reference 28, vide infra. The density of localized electron states is plotted as a function of their energy. Further simulations of this type to gather improved statistics would be valuable.
(32) Coe, J. V.; Earhart, A. D.; Cohen, M. H.; Hoffman, G. J.; Sarkas; H. W.; Bowen; K. H. *J. Chem. Phys.* **1997**, *107*, 6023.
(33) Bursulaya, B. D.; Jeon, H. J.; Yang, C.-N.; Kim, H. J. *J. Phys. Chem. A*, in press.
(34) Bursulaya, B. D.; Jeon, H. J.; Zichi, D. A.; Kim, H. J *J. Chem. Phys*. **1998**, *108*, 3286.
(35) Calculated from a Born−Haber cycle using standard enthalpies tabulated in Lias, S. G.; Bartmess, J. E.; Liebman, J. F.; Holmes, J. L.; Levin, R. D.; Mallard, W. G. *J. Phys. Chem. Ref. Dat., Supplement 1* **1988**, 17, 1.
(36) Fox, M. F.; Hayon, E. *J. Phys. Chem.* **1972**, *76*, 2703.
(37) Vedamuthu, M.; Singh, S.; Robinson, G. W. *J. Phys. Chem.* **1996**, *100*, 3825.
(38) Williams, F.; Varma, S. P.; Hillenius, S. *J. Chem Phys.* **1976**, *64*, 1549.
(39) Han, P.; Bartels, D. M. *J. Phys. Chem.* **1992**, *96*, 4899.
(40) Blandamer, M. J.; Fox, M. F. *Chem. Rev.* **1970**, *70*, 59.
(41) Borgis, D.; Staib, A. *J. Chem. Phys.* **1996**, *104*, 4776.
(42) Staib, A.; Borgis, D. *J. Chem. Phys*. **1996**, *104*, 9027.
(43) Sheu, W.-S.; Rossky, P. J. *Chem. Phys. Lett*. **1993**, *213*, 233.
(44) Sheu, W.-S.; Rossky, P. J. *J. Phys. Chem.* **1996**, *100*, 1295.